Journal of Colloid and Interface Science **228,** 263–269 (2000)
doi:10.1006/jcis.2000.6951, available online at http://www.idealibrary.com on IDEAL®

Dynamics of Capillary Rise

B. V. Zhmud,[1] F. Tiberg, and K. Hallstensson

Institute for Surface Chemistry YKI, Box 5607, Stockholm SE-11486, Sweden

Received October 4, 1999; accepted May 8, 2000

An overview and detailed analysis of the classical theory of capillarity is presented. A number of known equations of capillary rise dynamics are shown to be different limiting cases of one rather general equation. Some internal inconsistencies of the classical equations are pointed out. The role of nonlinear dissipation and flow pattern effects in the front zone of the liquid column and near the capillary entrance is discussed. Numerical simulations and experimental data demonstrating some characteristic types of dynamic behavior predicted by the theory are reported. Special attention is paid to the capillary rise of surfactant solutions. As applied to this special case, the existing theory is substantially elaborated by setting up a closed system of equations describing the surfactant transport and relaxation processes in the adsorption layer. A simplified relation for the capillary rise dynamics in the case of strong depletion of the interfacial region is obtained, which is in qualitative agreement with the experimental behavior.

Key Words: **capillarity; Lucas–Washburn equation; surfactants.**

INTRODUCTION

Many natural processes and human activities largely rely on the phenomenon of capillarity, i.e., the ability of liquids to penetrate into fine pores and cracks with wettable walls and be displaced from those with nonwettable walls. It is the capillarity that brings water to the upper layer of soils, drives sap in plants, or lays the basis for operation of pens. Knowledge of capillarity laws is important in oil recovery, civil engineering, dyeing of textile fabrics, ink printing, and a variety of other fields. This explains the continuous interest in the subject from the side of industry and fundamental science. Basic understanding of the capillarity laws was gained almost a century ago (1–5). Since then, the Lucas–Washburn equation has been serving for decades as the basis for describing the capillary phenomena (6–8). Unfortunately, as often happens with classical equations, the underlying assumptions this equation rests on are not always kept in mind in its applications. In such cases, an apparent agreement with experiment may be quite misleading. An instructive example is that the Lucas–Washburn equation predicts that the capillary rise should be proportional to the square root of time (in the short-time limit). The same kind of time dependence, being characteristic of diffusion-controlled processes, is often observed for surfactant solutions in hydrophobic capillaries (9–12). However, as will be shown later, the physics of these phenomena are completely different, and in the latter case, the Lucas–Washburn equation may not be applicable at all. The Lucas-Washburn equation also becomes inadequate in the zero-time limit, when the type of behavior it predicts appears to be nonsensical from a physical viewpoint, conflicting with the fundamental laws of mechanics and hydrodynamics (3, 4, 13, 14).

The goal of this paper has been to give an account of the physical concepts that make up the basis of the classical theory of capillarity. It shows that many familiar equations of capillary rise dynamics can be obtained as particular limiting cases of a more general—and pretty intuitive—equation. Several asymptotic regimes of the latter are investigated. The paper also sets up a theoretical framework suitable for description and modeling of capillary phenomena in surfactant solutions.

EXPERIMENTAL

Materials

Capillaries. The capillaries used in the experiments were precision bore borosilicate glass capillaries from Sigma–Aldrich (radii: 0.1, 0.15, 0.25, and 0.5 mm). Before measurements, the capillaries were cleaned with bichromate/sulphuric acid solution, rinsed with Millipore water, and dried in clean air atmosphere at 105°C. Hydrophobic capillaries were obtained by exposing (for several hours) the clean glass capillaries to dimethyl octyl chlorosilane (Fluka; purity, >97%) reacting with the silanol groups present at the surface of glass at room temperature. The hydrophobized capillaries were thoroughly rinsed with tetrahydrofuran and ethanol and dried at 105°C.

Chemicals. *n*-Dodecane (GC; purity, >99%) and diethyl ether (HPLC; purity, 99.9%) also were purchased from Sigma–Aldrich and used without further purification. Hexaethylene glycol monoalkyl ethers, C_nE_6, with decyl ($n = 10$) and myristyl ($n = 14$) chains, were purchased from Nikko Chemicals and used as received. Ethoxylated trisiloxane surfactants, $((CH_3)_3SiO)_2Si(CH_3)(CH_2)_2(OCH_2CH_2)_nOH$, also known as M(D′$E_n$)M superspreaders, were kindly provided by Dow Corning Corporation.

Methods

The capillary rise dynamics was followed from the moment the capillary was put in contact with the liquid. The liquid

[1] To whom correspondence should be addressed.

0021-9797/00 $35.00

was placed in a cylindrical glass dish filled slightly over the rim (thanks to the surface tension) to allow imaging immediately from the moment the capillary touches the liquid. However, when studying the rise of diethyl ether, a square-shaped ($5 \times 5 \times 10\,cm^3$) beaker was used instead of the cylindrical dish to minimize surface fluctuations. Fast rise processes were monitored with a high speed camera (Kodak Motion Corder Analyzer SR-1000) connected to a digital video recorder DVCAM DSR-V10P (Sony). The camera can capture up to 1000 frames per second. Slower processes were followed with a standard CCD video camera. The images were analyzed with NIH Image software SXM.

RESULTS AND DISCUSSION

I. Pure Liquids

I.1. Fundamental Equation of Dynamics

As applied to a viscous noncompressible liquid in a long cylindrical capillary, the Newton dynamics equation reads

$$\rho[zz'' + (z')^2] = \frac{2}{r}\gamma\cos\theta - \frac{8}{r^2}\eta z z' - \rho g z, \qquad [1]$$

where ρ is the density,[2] η is the viscosity, γ is the surface tension, θ is the wetting angle of the liquid, z is the height of capillary rise, r is the capillary radius, and g is the acceleration of gravity. This equation assumes the Poiseuille flow profile throughout the capillary. The capillary liquid will rise to a stationary level, z_∞, established by the balance of gravity and capillarity,

$$z_\infty = \frac{2\gamma\cos\theta}{\rho g r}. \qquad [2]$$

Discussing the dynamics of capillary rise, it seems natural to take $z(0) = z'(0) = 0$ as the initial conditions for Eq. [1]. However, because the above equation has a singularity at $t = 0$, when a finite force is applied to an infinitesimal mass, $m = \pi r^2 \rho z (z \to 0)$, this would lead to an ill-posed problem. A formal remedy is to take $z'(0) = \sqrt{2\gamma\cos\theta/\rho r}$ (4), neglecting such a logical drawback as the acceleration of liquid front at zero time being infinite. This impossible prediction of an initial infinite acceleration was removed by Szekely *et al.* (13) by composing the correct energy balance for the entry flow. Another roundabout way is to rewrite the first term on the left-hand side of Eq. [1] in the form

$$\rho(z + \lambda)z'', \qquad [3]$$

where λ stands for some effective initial height. The necessity for introducing such a correction, as well as the meaning and order of magnitude of λ, becomes clear on taking into account the flow continuity constraint, $\mathrm{div}(v) = 0$, where v is the velocity of the liquid. As a consequence of this constraint, the volume of liquid set into motion at the very beginning of capillary rise is not limited to the (infinitesimal amount of) liquid that is actually lifted above the zero level: the liquid present in the dipped part of the capillary, and in the bulk reservoir the capillary is connected to, starts moving at the same time.

The volume of liquid sucked into capillary from the bulk reservoir is equal to the volume passed through a closed surface drawn around the entrance point. Thus, assuming that the capillary just touches the liquid surface, that is, the length of the dipped part is negligible compared to the anticipated lift, the flow through the capillary cross section has to be equal to the flow through the surface of a hemisphere of radius R centered in the entrance point,

$$\pi r^2 v_{\text{cross-sect.}} = 2\pi R^2 v_{\text{sphere}}. \qquad [4]$$

Consequently, $|v_{\text{sphere}}|$ decays as R^{-2}, and the density of the kinetic energy as R^{-4}, which guarantees that the volume integral $\int v_{\text{sphere}}^2\,d\tau$ exists. This also suggests defining λ by

$$\lambda = \frac{\int v_{\text{sphere}}^2\,d\tau}{\pi r^2 v_{\text{cross-sect.}}^2} \propto r, \qquad [5]$$

which shows that the lower bound of the mass set into motion as the capillary rise commences is of the order of magnitude of $m = \pi r^3 \rho$. This simple argument showing that the capillary force always acts on a finite mass eliminates the initial burst.

I.2. Different Asymptotic Regimes

i. Quasi-steady stage (Lucas–Washburn equation). The Lucas–Washburn equation refers to a steady process, where the capillary force is compensated by gravity and viscous drag (1–2):

$$\frac{2}{r}\gamma\cos\theta - \frac{8}{r^2}\eta z z' - \rho g z = 0. \qquad [6]$$

The asymptotic solution corresponding to the short-time limit ($t \to 0$) is given by

$$z(t) = \sqrt{\frac{r\gamma\cos\theta}{2\eta}\,t} \quad (t \to 0), \qquad [7]$$

and predicts burst-like behavior with the velocity being infinite at zero time. This singularity of the solution highlights a deep inconsistency of the above equation. First, it is assumed that there is a steady laminar flow, and then, based on this assumption, a nonsensical conclusion is drawn that the velocity of the flow has to be infinite at zero time (13). It is well known that a fluid flow ceases being laminar as the velocity exceeds a certain limiting value, when an abrupt change in turbulence occurs. For a turbulent flow, the viscous drag is a nonlinear function of velocity, which necessitates that higher order terms in z' be included. Doing so results in a $z(t) \propto t^{(n/n+1)}$ short-time asymptotics where $n > 1$. Consequently, the slope of the z vs t plot becomes less severe as compared to that predicted by Eq. [7], although a weak singularity at zero time still persists. The latter is only gone on

[2] Rigorously speaking, the difference between the densities of the capillary liquid and air should be used; in most cases, the error will be negligible (ca. 0.1%).

taking into account the inertia terms (i.e., using Eq. [1] with the correction [3]).

The asymptotic solution corresponding to the long-time limit, i.e., when the liquid is about to approach its stationary level, z_∞ (see Eq. [2]), can be obtained as follows. Rewrite the Lucas–Washburn equation as

$$\frac{4}{r^2}\eta\frac{\mathrm{d}}{\mathrm{d}t}(z^2)+\rho g z=\frac{2}{r}\gamma\cos\theta \qquad [8]$$

and express the solution in the form

$$z(t)=z_\infty-\varepsilon(t). \qquad [9]$$

If the departure, ε, of the column height, z, from z_∞ is small, then $(z^2)'\cong -2z_\infty\varepsilon'$, and the resulting linear equation for ε is easily solved, leading to

$$\varepsilon(t)=\text{const}\cdot\exp\left(-\frac{\rho g r^2}{8\eta z_\infty}t\right). \qquad [10]$$

The preexponential factor should be chosen so that $\varepsilon(0)=z_\infty$; hence, finally, the following relaxation law results,

$$z(t)=z_\infty\left[1-\exp\left(-\frac{\rho g r^2}{8\eta z_\infty}t\right)\right]\quad(t\to\infty). \qquad [11]$$

Both asymptotic solutions obtained are compared with the exact (numerical) solution in Fig. 1.

ii. Low-viscosity limit (Quéré equation). For inviscid liquids, the fundamental equation [1] is reduced to (15, 16)

$$\rho[zz''+(z')^2]=\frac{2}{r}\gamma\cos\theta-\rho g z. \qquad [12]$$

Suppose that, in the vicinity of zero, the solution to the above equation is represented by an analytical function. Then, it can be approximated by a polynomial,

$$z(t)\cong P_n(t)=z_1t+z_2t^2+\cdots+z_nt^n. \qquad [13]$$

By substituting the latter into Eq. [12], one can see that the left-hand side contains powers up to and including $2n-2$, while the right-hand side has powers up to and including n. There is no discrepancy if and only if $n=2$. Thus, the solution is

$$z(t)=z_1t+z_2t^2$$
$$z_1=\sqrt{\frac{2\gamma\cos\theta}{\rho r}},\quad z_2=-\frac{g}{6}, \qquad [14]$$

which shows that there is an inversion point, where the velocity changes its sign. The solution is periodical with a period $T=z_1/z_2$. The proof is straightforward. Substitute $z(t+z_1/z_2)$ into Eq. [15]. Since $z(t)$ has already been proven to be a solution, it only remains to prove that the equality $6z_1^2+6z_1z_2t=-g[z_1^2/z_2+z_1t]$ holds for any t. This requires that $6z_1z_2=-gz_1$ and $6z_1^2=-gz_1^2/z_2$, which is certainly satisfied for z_1 and z_2 defined in Eq. [14].

The existence of oscillations can also be proven in a different way. Assume that the equilibrium level is slightly perturbed, so that $z(t)=z_\infty+\varepsilon(t)$, where the perturbation, ε, is small. Then it is easy to see that $\varepsilon(t)$ has to meet the equation

$$\varepsilon''+\frac{g}{z_\infty}\varepsilon=0, \qquad [15]$$

describing harmonic motion with frequency $\omega=\sqrt{g/z_\infty}$. Similar arguments show that for low-viscous liquids, damping oscillations should be observed, as confirmed by the direct numerical solution of Eq. [1] discussed next. Continuous oscillations of liquid level just reflect the fact that no dissipation of energy is allowed for (an exchange with the reservoir prevents the conservation of energy of the capillary liquid even if $\eta=0$).

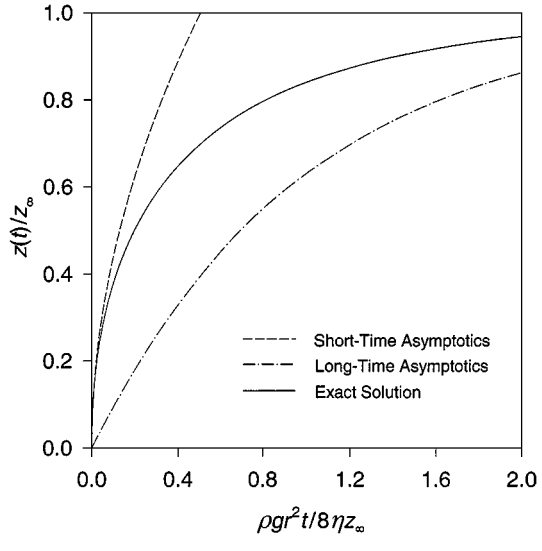

FIG. 1. Comparison between the exact solution of the Lucas–Washburn equation and its short- and long-time asymptotics.

I.3. Numerical Analysis

It is convenient first to rewrite Eq. [1] in the form

$$\rho[(z+\lambda)z''+(z')^2]+Vzz'+\rho g z=F, \qquad [16]$$

where $V=8/r^2$ and $F=\gamma\cos\theta/r$ reflect the relative contributions of viscous drag and capillary force, respectively.

The solution of Eq. [16] can be carried out numerically through finite differences. A few remarks concerning the initialization of the finite-difference procedure need to be stated. Let h be the integration step size. From the initial conditions, it follows that $z(0)=z(h)=0$, so that

$$z(2h)=2\left(-\lambda+\sqrt{\lambda^2+h^2\frac{F}{\rho}}\right)\cong\frac{Fh^2}{\rho\lambda^2}.$$

Therefore, h must be chosen small enough to ensure $z(2h)\ll z_\infty$,

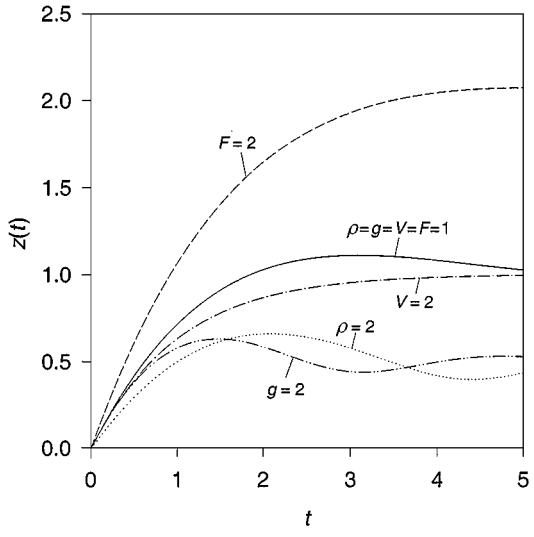

FIG. 2. Numerical solutions to the fundamental dynamic equation [16] for different values of parameters.

i.e., $h \ll \lambda/g^{1/2}$. However, to be sure that the amount of liquid being accelerated does not change appreciably, an additional constraint is required, $h \ll \lambda$. This also provides additional evidence that the problem would be ill-posed if $\lambda = 0$.

Figure 2 shows, at a qualitative level, the influence of different parameters entering Eq. [16] on the dynamics of capillary rise. Initially, the liquid sucked into the capillary is accelerated by capillary force ($z \sim t^2$); however, soon thereafter the capillary force is compensated for by the viscous drag so that a quasi-steady state is achieved ($z \sim t^{1/2}$), and eventually the rise is slowed down by gravity. It should once again be emphasized that the viscous drag is the only factor damping oscillations in this model. In practice, there is additional dissipation of energy by liquid returned to the bulk reservoir, so the damping will be faster than predicted.

I.4. Comparison with Experiment

The experimental data on capillary rise dynamics of dodecane in glass capillaries have been fitted by using Eq. [6], Eq. [1], and Eq. [1] augmented by including the turbulent drag

$$\Phi = \begin{cases} 0 & (|z'| < v_{cr}) \\ qz(z')^2 & (|z'| > v_{cr}), \end{cases} \qquad [17]$$

which will appear in the form $-\Phi/r^2$ on the right-hand side of Eq. [1]. Here, v_{cr} is the barrier velocity when the turbulence begins, and q is some coefficient. The results are compared in Figs. 3a and 3b. Although all three equations give similar results at relatively long times, only the third one of them proves to be adequate in the short-time limit. The dissipation of energy becomes much greater when the turbulence begins, slowing down the flow rate. An important remark needs to be stated in this connection: the best fit to the experimental data is obtained if the critical velocity is taken to be ca. 0.04 m s^{-1}. This corresponds to the Reynolds number $R_e \sim 2$, which seems too low for turbulence to occur (17). Thus, the word "turbulence" should be used with caution. Apparently, the term [17] simply corrects for some second-order dissipation effects related to the complexity of the actual flow pattern near the meniscus at the moment the liquid is entering the capillary. Besides a better agreement with the experiment, the major improvement achieved when allowing for these nonlinear drag and inertia terms is that the resulting dynamic equation, in contrast with the Lucas–Washburn equation, has no singularity at zero time.

Thus far, it has been neglected that in order to fill a capillary, the capillary liquid has to displace another fluid, usually air or vapor. Taking this into account would result in additional dissipation of energy; the corresponding viscous drag being

$$8\pi\eta_g(L - z)z', \qquad [18]$$

where η_g is the viscosity of the displaced fluid, and L is the capillary length. The effect can be significant for low-viscous liquids. An instructive example can be seen in Fig. 4 showing the capillary rise dynamics of diethyl ether, one of few liquids where damping oscillations of liquid level are expected. Based on the physical parameters of this fluid, the oscillations are possible if the aspect ratio, r/z_∞, is greater than approximately 0.05. In particular, for $r = 0.5$ mm, the theory based on Eq. [1] predicts pretty large oscillations. Experimentally, such oscillations are observed only for short capillaries ($L = 5$ and 10 cm). The amplitude of oscillations decreases with increasing the capillary length, and for capillaries 30 cm long, the oscillations turn

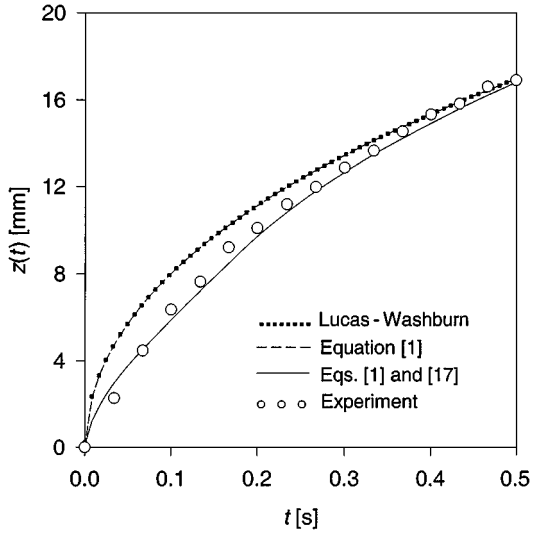

FIG. 3. Experimental data for dodecane fitted according to the Lucas–Washburn equation [6] (···), the basic equation [1] (– – –), and Eq. [1] augmented by including the nonlinear drag [17] (——). The following values of parameters have been used: $\eta = 1.7 \times 10^{-3}$ (the first two equations) and 1.5×10^{-3} (the last equation) Pa · s; $\rho = 750$ kg m^{-3}; $\gamma = 2.5 \times 10^{-2}$ N m^{-1}; $\theta = 17°$; $q = 0.3$ kg m^{-2}; and $r = 10^{-4}$ m.

into a single overshot over the equilibrium height, followed by damping to the equilibrium height. The fact that the amplitude of oscillations is significantly reduced on allowing for the additional viscous drag due to the air being expelled from capillary by rising liquid is also confirmed by numerical simulations, although the amplitude of oscillations is somewhat overestimated, which becomes especially marked for long capillaries. This persisting discrepancy needs to be commented on in brief. First, it is possible that evaporation of ether during the experiment cools the capillary down, thus rendering the capillary liquid more viscous. As can be seen in Fig. 4, using $\eta = 0.6$ mPa · s, which would correspond to a temperature well below 0°C, instead of $\eta = 0.22$ mPa · s, the viscosity at the normal temperature, gives much better agreement with the experiment. However, this argument falls short and should be rejected if the experiment has been carried out in a saturated vapor atmosphere, e.g., in prewetted capillaries. Alternatively, a perfect fit to the experimental data can be obtained by making allowances for the second-order dissipation effects as reflected in Eq. [17]. Finally, it should be kept in mind that all the above equations neglect the extreme complexity of the actual flow pattern near the ends of the capillary and in the vicinity of the meniscus. Indeed, laminar flows in a pipe are characterized by a parabolic velocity profile with the zero velocity at the walls (the no-slip condition). This also holds true for a capillary flow. Far from the meniscus, there exists no

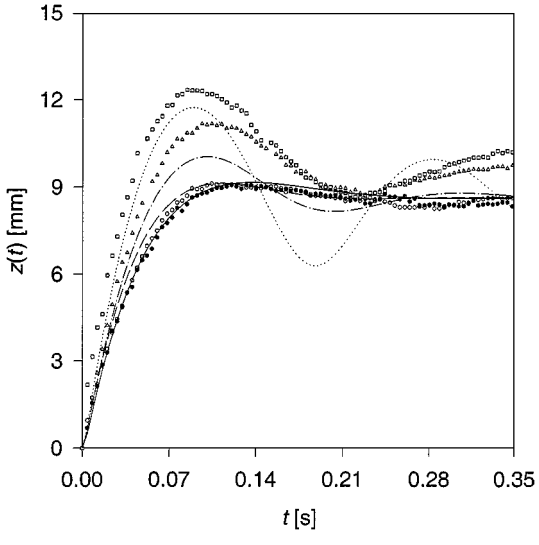

FIG. 4. Experimental results: Capillary rise dynamics of diethyl ether in glass capillaries of radius $r = 5 \times 10^{-4}$ m and length $L = 0.05$ m (□), 0.1 m (△), and 0.3 m (○ and ●); the last measurement was done with dry (○) and prewetted (●) capillaries. Simulation results: (···) the theoretical curve calculated by Eq. [1]; (– · –) the theoretical curve calculated by Eq. [1] augmented by taking into account the viscosity of air (Eq. [18]); (– – –) the theoretical curve calculated by setting $\eta = 6 \times 10^{-4}$ Pa · s to simulate of the capillary cooling effect; and (——) the best-fit curve obtained by using Eq. [1] with corrections [17] and [18]. Unless otherwise stated, the following physical constants were used (25): $\eta = 2.2 \cdot 10^{-4}$ Pa · s, $\eta_b = 1.86 \times 10^{-5}$ Pa · s, $\gamma = 1.67 \times 10^{-2}$ N m^{-1}, and $\rho = 710$ kg m^{-3}. The wetting angle $\theta = 26°$ was fitted to correctly reproduce the experimental rise height, $z_\infty = 8.6 \times 10^{-3}$ m, in equilibrium.

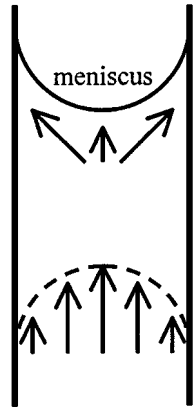

SCHEME 1

radial component of the velocity vector, since the walls are nonpenetrable. However, it is clear that scaling this convex velocity profile with time could not produce a concave meniscus unless there were a lateral flow in the head zone. This situation is depicted in Scheme 1. The hydrodynamics of the fluid motion in the reservoir near the capillary entrance and the departure from Poiseuille flow in the vicinity of the advancing meniscus were studied by Levine *et al*. who developed a comprehensive mathematical theory of these effects (18, 19). Since the length of the head zone does not exceed a few radii, these effects can safely be neglected for fine capillaries. Yet when it comes to capillary oscillations, rather wide capillaries are required, and here, the aforesaid effects, as well as the related effects of surface tension and contact angle relaxation, may be of importance.

II. Surfactant Solutions

It is the adsorption of surfactant to the capillary walls that makes possible the rise of surfactant solutions in hydrophobic capillaries. In the absence of surfactant, the capillary depression would rather occur. If either (i) the transport of solute is very fast and the adsorption to the walls is slow or (ii) the transport and the adsorption are both fast, but the amount adsorbed to the walls is small, then the surface excess of surfactant at the gas/liquid interface and, therefore, the surface tension and the capillary force as well almost do not change with time. It is the only case where the classical theory of capillary reviewed in the previous section is applicable. Of the above-mentioned regimes, the first can be realized if the capillary walls are wettable without preadsorption surfactant and the second can be realized for sufficiently viscous liquids, wide capillaries, and wetting angles close to 90°, i.e., when the capillary's cross-section-to-wall area ratio is not too small, and, finally, for concentrated surfactant solutions. Herewith, it is assumed that the lateral transport of surfactant along the gas–liquid interface and the surface tension relaxation are sufficiently fast.

The next case where the diffusional transport of solute is a rate-determining stage warrants special consideration. This case is pertinent to studies of surfactant-induced capillary phenomena

in hydrophobic materials. To keep the problem tractable, the following additional assumptions will be made: (i) the capillary rise commences when a certain amount of surfactant has been adsorbed on the capillary wall; (ii) the surfactant is transferred to the wall mainly from a thin interfacial zone (adsorption zone) where the surfactant concentration is much higher than in the bulk solution; and (iii) the adsorption at the solid/liquid interface is irreversible. Thus, the transport of surfactant in the front zone is given by the sum of incoming and outgoing fluxes

$$\frac{d\Gamma_{gl}}{dt} = \frac{j_+ + j_-}{\pi r^2}$$
$$j_+ = -D\frac{\partial c}{\partial \zeta}\bigg|_{\zeta=z(t)} \cdot \pi r^2 \qquad [19]$$
$$j_- = -2\pi r z' \Gamma_{sl}^m \left\{1 - \exp\left(-\frac{k_{sl}^+ \Gamma_{gl}}{\Gamma_{sl}^m z'}\right)\right\},$$

where Γ is the magnitude of adsorption, D is the diffusion coefficient of surfactant in solution, k^+ is the adsorption rate constant, and the subscripts gl and sl refer to the gas/liquid and solid/liquid interface, respectively. Adsorption affinity of surfactant to the solid surface is assumed to be sufficiently high, so that Γ_{sl} tends to the monolayer capacity, Γ_{sl}^m, with increasing the exposure time (which is inversely proportional to the front zone velocity, z').

A rigorous treatment of the problem requires solution of the dynamic equation [1] coupled with the diffusion equation

$$\frac{\partial c}{\partial t} = D\frac{\partial^2 c}{\partial \zeta^2} - z'\frac{\partial c}{\partial \zeta} \quad (0 < \zeta < z) \qquad [20]$$

under appropriate boundary conditions (20) imposed on the functions $c(\zeta, t)$ and $z(t)$. The coupling is effected through the capillary force term, $\gamma(t)\cos\theta(t)$, which is related to the concentration of surfactant in the vicinity of the gas/liquid interface and the adsorption kinetics at the gas/liquid and solid/liquid interfaces.

Given the order of magnitude of the diffusion coefficient in liquids and the characteristic capillary filling times, a meaningful assumption is that the length of the diffusion zone is much smaller than z and scales as $(Dt)^{1/2}$ with time. Hence, the concentration gradient near the gl interface is approximately equal to $c_b/(Dt)^{1/2}$, where c_b is the bulk concentration of surfactant. Within certain time limits, the capillary rise represents a quasisteady process, where the amount of surfactant adsorbed to the solid/liquid interface per unit time is equal to that transported to the gas/liquid interface by diffusion,

$$2\pi r \Gamma_{sl}^m \, dz \approx \pi r^2 D \frac{c_b}{(Dt)^{1/2}} \, dt, \qquad [21]$$

which leads to the following scaling relation,

$$z(t) \approx \frac{r c_b}{\Gamma_{sl}^m}(Dt)^{1/2}. \qquad [22]$$

Thus, if the interfacial region becomes strongly depleted of surfactant, the rise rate is limited by diffusional transport of surfactant to the interface. In this case, the same time dependence, $z(t) \sim t^{1/2}$, as predicted by the Lucas–Washburn equation is observed, but the latter is inapplicable here.

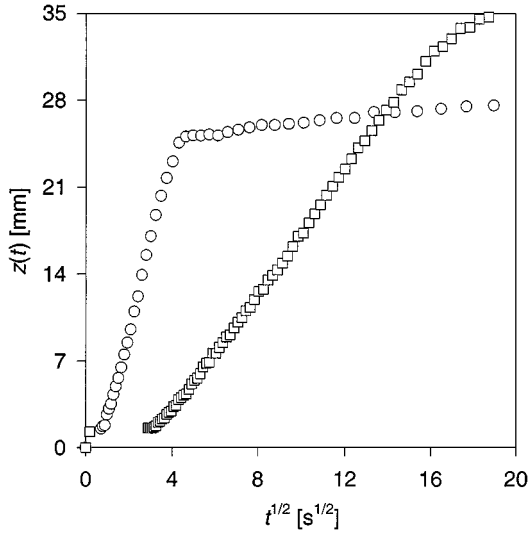

FIG. 5. Capillary rise dynamics of 1 mM $C_{10}E_6$ (○) and $C_{14}E_6$ (□) surfactant solutions in hydrophobic capillaries ($r = 10^{-4}$ m).

As can be seen in Fig. 5, the experimental z vs $t^{1/2}$ curves really have a nearly linear part (usually after some induction period needed for the capillary force to build up), showing that the rate of filling is limited by diffusional transport of surfactant to the interface.

Any change in the amount of surfactant adsorbed at the gas/liquid interface will in general cause some change in the surface tension in accord with the Gibbs equation

$$\gamma = \gamma_0 - RT \int_{c=0}^{c=c(z,t)} \Gamma_{gl} \, d\ln c. \qquad [23]$$

It is the surface tension relaxation that is responsible for overshooting the equilibrium rise height by surfactant solutions. This kind of behavior is demonstrated in Fig. 6. It is easy to prove that this overshot is noninertial by its nature: it can exist even in a quasi-steady state (Lucas–Washburn equation). Let the surface tension relax according to the simple law

$$\gamma = \gamma_0 - \Delta\gamma\varphi_\beta(t), \qquad [24]$$

where

$$\Delta\gamma = \gamma_0 - \gamma_\infty \quad \text{and} \quad \varphi_\beta(t) = 1 - \exp(-\beta t). \qquad [25]$$

Here, γ_0 is the initial surface tension, γ_∞ is the equilibrium surface tension, and β is the relaxation rate constant. Substituting the latter expression into Eq. [6] and differentiating by time gives

$$-\frac{2\beta\Delta\gamma\cos\theta}{r}\exp(-\beta t) = \frac{8\eta}{r^2}[(z')^2 + zz''] + \rho g z'. \qquad [26]$$

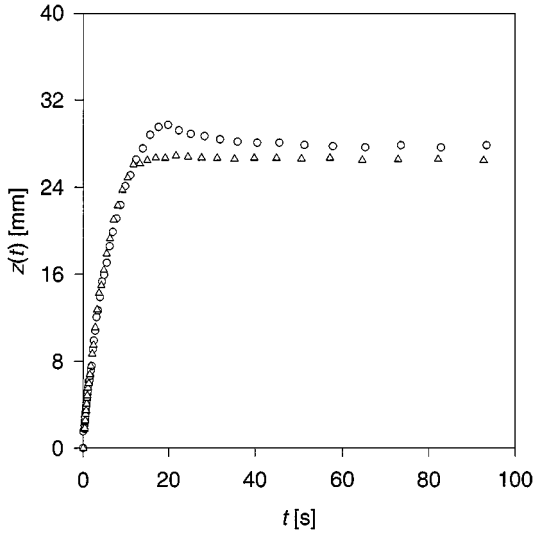

FIG. 6. Capillary rise dynamics of 0.01 M (○) and 0.02 M (△) aqueous solutions of ethoxylated trisiloxane surfactant, M(D′E$_6$)M, in 0.15-mm glass capillaries. The maximum disappears at a higher concentration of surfactant, as the surface tension relaxation rate increases with concentration.

If the height is a maximum, $z'|_{t=t_m} = 0$, and $z''|_{t=t_m} < 0$, then

$$-\beta\Delta\gamma\cos\theta\exp(-\beta t_m) = \frac{4\eta}{r}zz''\Big|_{t=t_m}. \qquad [27]$$

Notice that both sides of the above equation have the same sign. As $t \to 0$, the expression on the left-hand side tends to a constant, $\beta\Delta\gamma\cos\theta$, while the expression on the right-hand side goes to infinity as t^{-1}. In the opposite limit, as $t \to \infty$, both sides relax to zero exponentially; for the right-hand side the relaxation law being $\exp(-\alpha t)$ with $\alpha = \rho g r^2/8\eta z_\infty$. For a real root to exist, the plots of the right-hand side and the left-hand side versus time must intersect. This is only possible if $\beta < (\text{const})\alpha$, whence a conclusion is drawn that the relaxation must not be very fast as compared to the capillary filling in order for a maximum to occur. The numerical analysis supports this conclusion (see Fig. 7).

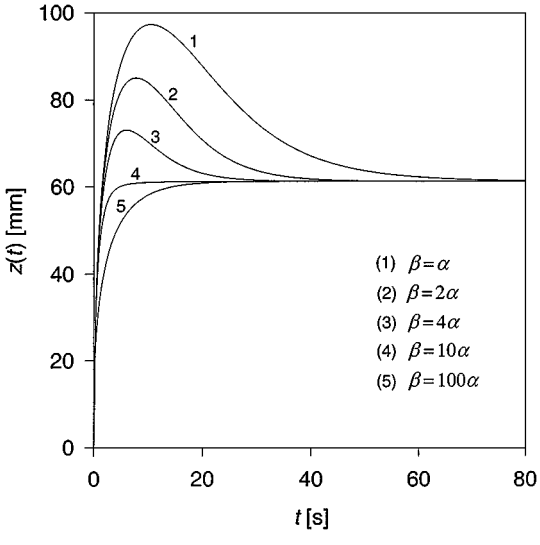

FIG. 7. Simulated capillary rise dynamics for aqueous solutions of (hypothetical) surfactants that cause the surface tension relaxation from $\gamma_0 = 7.2 \times 10^{-2}$ N m^{-1} to $\gamma_\infty = 3.0 \times 10^{-2}$ N m^{-1} with the relaxation rate constant, β, varying from 1α up to 100α ($\alpha = 8.33 \times 10^{-2}$ s^{-1}). Other parameters were as follows: $r = 10^{-4}$ m, $\eta = 10^{-3}$ Pa · s, $\rho = 1000$ kg m^{-3}, and $\theta = 0°$. Under the conditions specified, no maximum at the $z(t)$ curve is possible if the surface tension relaxation time, $1/\beta$, is less than approximately 1.2 s.

The situation becomes more complex in concentrated surfactant solutions, where the transport properties of surfactant are affected by interconversation between the molecular and micellar forms of surfactant (21, 22). Furthermore, it should be kept in mind that, apart from surfactant adsorption, there exist other factors influencing the contact angle and surface tension dynamics (23, 24).

ACKNOWLEDGMENTS

This work was supported by the Swedish Foundation for Strategic Research and the Swedish Pulp and Paper Research Foundation.

REFERENCES

1. Lucas, R., *Kolloid Z.* **23,** 15 (1918).
2. Washburn, E. W., *Phys. Rev.* **17,** 273 (1921).
3. Rideal, E. K., *Philos. Mag. Ser. 6* **44,** 1152 (1922).
4. Bosanquet, C. H., *Philos. Mag. Ser. 6* **45,** 525 (1923).
5. Marmur, A., *in* "Modern Approach to Wettability: Theory and Applications" (M. E. Schader and G. Loeb, Eds.), p. 327. Plenum, New York, 1992.
6. Ligenza, J. R., and Bernstein, R. B., *J. Am. Chem. Soc.* **73,** 4636 (1951).
7. Fisher, L. R., and Lark, P. D., *J. Colloid Interface Sci.* **69,** 486 (1979).
8. Malik, R. S., Laroussi, C. H., and de Becker, L. W., *Soil Sci.* **127,** 211 (1979).
9. Lenher, S., and Smith, J. E., *Am. Dyest. Rep.* **22,** 689 (1933).
10. Caryl, C. R., *Ind. Eng. Chem.* **33,** 731 (1941).
11. Folkes, F. M., *J. Phys. Chem.* **57,** 98 (1953).
12. Hodgson, K. T., and Berg, J. C., *J. Colloid Interface Sci.* **121,** 22 (1988).
13. Szekely, J., Neumann, A. W., and Chuang, Y. K., *J. Colloid Interface Sci.* **35,** 273 (1971).
14. Levine, S., and Neale, G. H., *J. Chem. Soc. Faraday Trans. 2* **71,** 12 (1975).
15. Quéré, D., *Europhys. Lett.* **39,** 533 (1997).
16. Quéré, D., Raphael, E., and Ollitrault, J.-Y., *Langmuir* **15,** 3679 (1999).
17. Coulson, J. M., and Richardson, J. F., "Chemical Engineering," 2nd ed., Vol. 1. Pergamon, Oxford, 1965.
18. Levine, S., Reed, P., Watson, E. J., and Neale, G., *in* "Colloid and Interface Science" (M. Kerker, Ed.), Vol. III, p. 403. Academic Press, New York, 1976.
19. Levine, S., Lowndes, J., Watson, E. J., and Neale, G., *J. Colloid Interface Sci.* **73,** 136 (1980).
20. Tiberg, F., Zhmud, B., Hallstensson, K., and von Bahr, M., submitted for publication.
21. Fainerman, V. B., Rakita, Yu. M., and Zadara, V. M., *Zh. Fiz. Khim.* **58,** 2006 (1984).
22. Zhmud, B. V., Tiberg, F., and Kizling, J., *Langmuir* **16,** 2557 (2000).
23. de Gennes, P. G., *Rev. Mol. Phys.* **57,** 827 (1985).
24. Dussan, E. B., *Annu. Rev. Fluid Mech.* **11,** 371 (1979).
25. "CRC Handbook of Chemistry and Physics," 79th ed. (D. R. Lide, Ed.). CRC Press, Boca Raton, FL, 1998–1999.